

# Noise-based Underactuated Mobile Robot Inspired by Bacterial Motion Mechanism

Kazumichi Shirai and Yoshio Matsumoto and Yutaka Nakamura and Satoshi Koizumi and Hiroshi Ishiguro

**Abstract**—Living organisms have various kinds of flexibility and robustness which are realized by “yuragi,” i.e. biological fluctuations or noises. Bacterial motion is a form of noise-based motion, since bacteria can move towards a higher concentration of some chemical which they prefer even though they have only a limited 1-DOF of flagella for mobility. Bacteria also have only a limited sensory device which cannot detect the spatial gradient of the chemical at a time. The simple strategies that bacteria take to realize chemotaxis are (1) to tumble (or turn) to change orientation randomly with unbundled flagella in various directions being hit by surrounding water molecules, and (2) to change the frequency of tumbling according as the time change of chemical concentration. In this paper, we describe a small and simple, 1-DOF swimming robot developed by mimicking the bacterial motion generation mechanism. The robot only has a single motor and a single sensor (a photo detector), however, by changing its orientation in response to various noises which exist in the environment, and by changing the frequency of turning, the robot can approach its goal. Experimental results indicate that the robot statistically approaches the goal (a light source) in two dimensional space with its 1-DOF actuator, which would be impossible for the robot to achieve without utilizing noises in the environment.

**Index Terms**—Mobile Robot, 1-DOF, Chemotaxis, Bacteria, Noise

## I. INTRODUCTION

Living organisms have various kinds of flexibility and robustness which allow them to survive in real, complex and dynamic environments. Interpreting such mechanisms of organisms from the engineering point of view will lead to new control methods in robotics and simple but robust robots which work in the real world. Biologically-inspired robotics is one of the most active research fields in robotics for this reason[1].

There are numerous biological studies on the navigation methods of insects, and some of them have been applied to the navigation of mobile robots. For instance, a model of desert ants was implemented on Sahabot2[2], which visually memorizes snapshots of the environment for homing. By comparing the memorized snapshots with the current view, ants can determine the way back to their nest. Another research focused on the bee, which also utilizes visual information for homing[3].

In this research, we focus on a simpler microorganism, a bacterium, and develop a swimming robot mimicking the moving mechanism of a bacterium. A bacterium is one of the smallest and simplest organisms on earth. The actuator of bacterium is called a flagellum, which acts like

a propeller with a 1-DOF motor. The sensor of bacterium is also quite simple and can only detect the concentration of chemicals without gradient information. It is remarkable that bacteria can still navigate toward chemical stimulus (i.e. food) in 3D space, despite such simple structures for sensing and actuation. In contrast, it is trivial in robotics that a mobile robot equipped with 2-DOF actuators such as wheels can navigate in arbitrary direction in 2D space. It is also trivial that a mobile robot equipped with two sensors can estimate the gradient of sensed objects and thus perform goal orientation. Therefore it is easy to build a simple mobile robot that exhibits phototaxis utilizing two sensors and two actuators.

The rest of this paper is organized as follows: Section 2 describes how a bacterium realizes chemotaxis. In Section 3, the hardware and the software implementation is described. Experimental results and conclusions are shown in Section 4 and 5 respectively.

## II. MECHANISM OF CHEMOTAXIS OF BACTERIA

Some bacteria, such as *E. coli*, have several flagella (4-10 typically)[4]. Each flagellum has a tiny rotary motor at its base, however the motions of all flagella are synchronized, which means that a bacteria can only control flagella as a 1-DOF actuator. The flagella can rotate in two ways as follows[5], [6]:

- 1) Swimming mode: Counter-clockwise rotation aligns the flagella into a single rotating bundle, causing the bacterium to swim in a straight line (Fig. 1(A)).
- 2) Tumbling mode: Clockwise rotation breaks the flagella bundle apart so that each flagellum points in a different direction. This allows the bacterium to efficiently receive a random force of bombardment when each flagellum rotates, colliding with surrounding water molecules undergoing Brownian motion, causing the bacterium to tumble in place (Fig. 1(B)).

The overall movement of a bacterium is the result of alternating tumbling and swimming modes. Bacteria such as *E. coli* are unable to choose the direction in which they swim, and are unable to swim in a straight line for more than a few seconds due to rotational diffusion. In other words, bacteria “forget” the direction in which they are going.

Sensing of chemical gradients is also a crucial step in the process. A cluster of receptors for particular chemicals exists at the front part of *E. coli*. However, due to their small size, bacteria cannot effectively detect concentration gradients, therefore these cells scan and evaluate their environment by constant swimming (consecutive sequences of

Authors are with Graduate School of Engineering, Osaka University, 2-1, Yamadaoka, Suita, Osaka, 565-0879, Japan  
h.kwakernaak@autsubmit.com

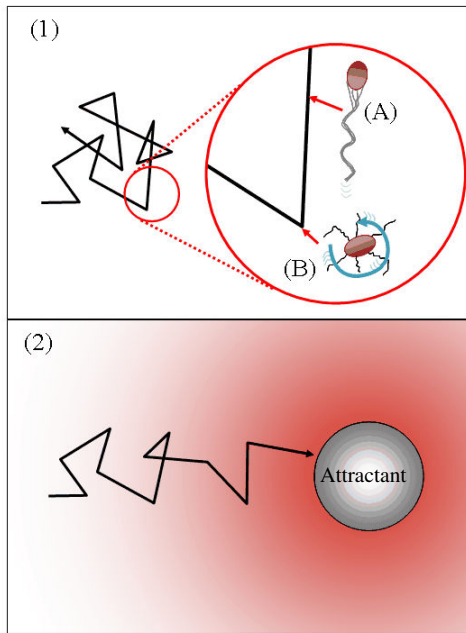


Fig. 1. (1) Random walk and (2) biased random walk toward attractant of a bacterium, both of which involve the (A) swimming mode and (B) tumbling mode

straight swimming and tumbling). Given these limitations, it is remarkable that bacteria can direct their motion to find favorable locations with high concentrations of attractants (i.e. nutrition) and avoid repellents (i.e. poisons).

When a bacterium is swimming in a uniform environment, the possibilities of action selection for “swimming” and “tumbling” are constant, and the movement would look like a random walk with relatively straight swims interrupted by random tumbles that reorient the bacterium[7] as shown in Fig. 1(1).

In the presence of a chemical gradient, bacteria exhibit chemotaxis, or direct their overall motion to the attractant based on the gradient[8], as shown in Fig. 1(2). If a bacterium senses that it is moving in the correct direction (toward an attractant or away from a repellent), it will keep swimming in a straight line for a longer time before tumbling, and if it is moving in the wrong direction, it will tumble sooner and try a new direction at random. In other words, bacteria like *E. coli* use temporal sensing to decide whether life is getting better or worse. In this way, they find the location with the highest concentration of attractant (usually the source) quite well as shown in Fig. 1(2). Fleeing from a repellent works with the same efficiency. It seems remarkable that this purposeful random walk is a result of simply changing the frequency of action selection from “tumbling” and “swimming” using a 1-DOF actuator with simple feedback from the sensor.

#### A. Navigation of Robot Inspired by Bacteria

Tsuji *et al.* proposed a navigation method based on the chemotaxis of bacteria[9]. They first modeled the processing mechanism of chemotaxis of *E. coli* and simulated the

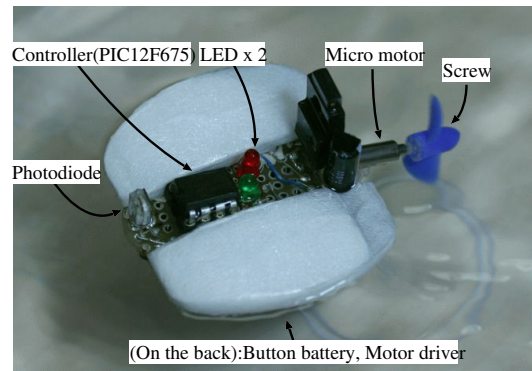


Fig. 2. Developed 1-DOF swimming robot

motion. In the simulation, motor commands were calculated based on the chemical concentration in the environment, and moving direction was determined. In addition, a genetic algorithm was applied in order to adjust some parameters in the model, so generated trajectories fit actual trajectories of the bacteria. Then they applied the acquired model of a bacterium to a mobile robot with two wheels and a photo sensor detecting the intensity of the floor[10], and showed that the robot was able to approach a dark colored area.

In contrast to this, we focus on the fact that bacteria can move in 3D space utilizing only a 1-DOF actuator. Thus the robot we develop has a single motor for moving forward and a single sensor to detect the light intensity, and the navigation mechanism that bacteria have in order to achieve a taxis toward the goal is implemented. How to achieve tumbling motion without an additional actuator is the key to realizing the navigation mechanism. In order to receive random, noisy forces from the environment, we implement the robot as a swimming robot in the water. In addition, we utilize a propeller to generate both forward motion for the robot and disturbed flows in the environment at the same time.

### III. 1-DOF ROBOT INSPIRED BY BACTERIA

#### A. Hardware

Fig. 2 shows the developed prototype of a 1-DOF swimming robot. A photo IC diode S7183 (Hamamatsu Photonics K.K.) is installed at the front of the robot as a sensing device for the light intensity. As a tiny processor, PIC12F675 (Microchip Technology Inc.) is adopted. A micro motor with a screw is attached to the hind part of the robot, and a motor driver IC TA7291P (Toshiba Corp.) is utilized for controlling the rotational direction of the motor. As floating buoyant material, Styrofoam parts are mounted at both sides of the robot. Two button-type lithium batteries are attached to the bottom of the robot. We used two LEDs in order to observe the sensing status of the robot.

#### B. Software

Since the robot only has a single photo detector, it cannot detect the spatial distribution of the lighting intensity. Therefore it has to determine the action to take according to the change over time of the lighting intensity as the bacteria do.

One of the following four actions is executed as a step of action of the robot:

- 1) When the change over time is large and positive, the motor rotates CCW for 1.5[s].
- 2) When the change over time is small and positive, the motor rotates CCW for 1.0[s].
- 3) When the change over time is nearly zero, the motor rotates in random direction (CCW or CW) for 0.7[s].
- 4) When the change over time is negative, the motor rotates CW for 0.3[s], and then stops for 0.3[s].

The times for motor rotation were determined experimentally in order to produce adequate motion. The change over time of the lighting intensity is defined as the difference between the current intensity and the intensity one step before. The long CCW rotation of the motor corresponds to swimming which moves the robot forward, while the instant short CW rotation subsequent to CCW rotation corresponds to tumbling which generates a disturbed flow in the liquid.

The causes of the environmental noises acting on the robot are considered to be as follows:

- disturbed flow of the liquid,
- wind and waves,
- collisions with the wall,
- vibration of the motor,
- asymmetric design of the robot.

When the motor rotates CCW and stops, these noises control the movement of the robot and cause it to change orientation.

### C. Evaluation Experiment

1) *Experimental Setup:* Fig. 3 shows the setup for the experiment. A circular tank of 35[cm] in diameter is utilized as a swimming field for the developed robot. The tank is filled with Flourinert<sup>TM</sup> (3M), which is an electrically insulating, inert fluorinated liquid usually utilized for cooling electronics. Due to the liquid's insulation characteristics, the robot is able to work in it without water proof processing. A small fluorescent light is installed at the outer side of the tank as the target. In order to prevent the effect of the reflection, the wall of the tank was all covered with black vinyl tape except for the fluorescent part. An IEEE1394 digital video camera DFW-VL500 (Sony Corp.) is installed above the center of the tank, and is utilized for visually recording the trajectory of the robot using a marker as well as the activity of the robot using LEDs.

2) *Swimming and Tumbling Motion:* To show the properties of the robot's movement, we recorded the trajectories of the robot for particular motions. Fig. 4 indicates the trajectories resulting from various combinations of swimming and tumbling motions, in which "S" indicates a swimming motion for 3.0[s], and "T" indicates a tumbling motion for 0.6[s] respectively. As shown in Fig. 4(1) the swimming motion not exactly straight. The tumbling motion makes the robot turn as shown in Fig. 4(2),(3) and (4). From these figures, the turning angle in tumbling motion may look the same every time. However as shown in Fig. 5 the angle is not exactly the same even when the robot executes the

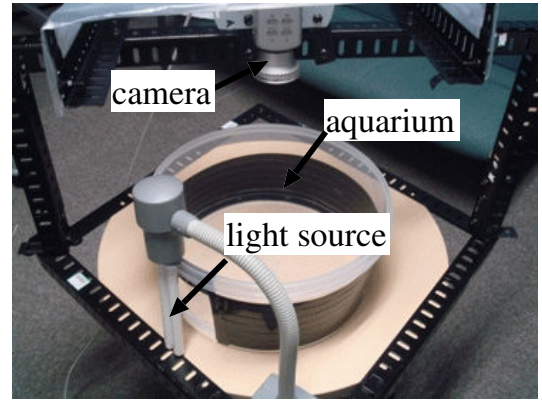


Fig. 3. Experiment environment for swimming robot

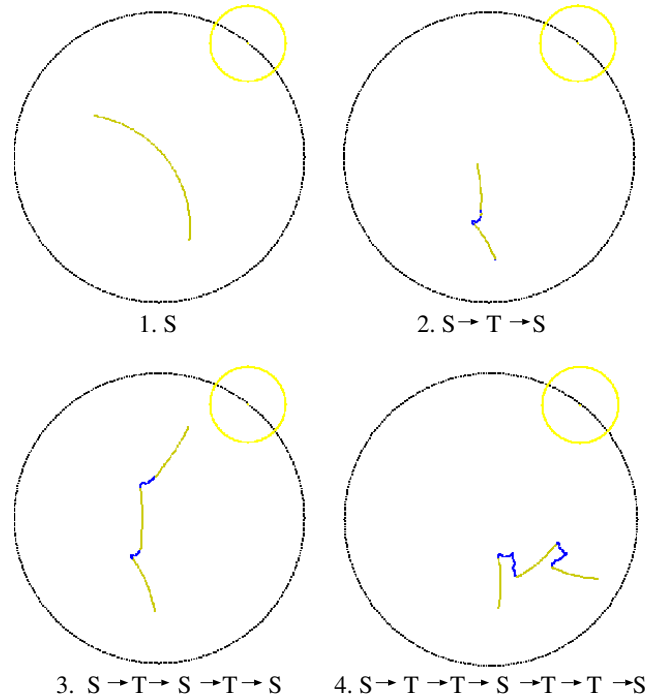


Fig. 4. Trajectories of basic motion sequences for the swimming robot

same motion sequence. In addition there are other causes which make the robot turn as described in Section III-B; therefore the resulting trajectory becomes more complex and unpredictable.

3) *Evaluation of Phototaxis:* In order to confirm the phototaxis of the robot, we conducted a navigation experiment. The robot was placed in the Flourinert at the center of the tank with a fixed initial pose (at a direction perpendicular to the light source). Ten trials of the navigation for 180[s] were conducted while recording the trajectories. Examples of the recorded trajectories are shown in Fig. 6. The light source as the attractant is located at the top right of the tank. The colors of the trajectory corresponds to the detected change over time of light intensity. Red, green, yellow, and blue means that the change over time of detected intensity is large and positive, small and positive, around zero, and negative respectively.

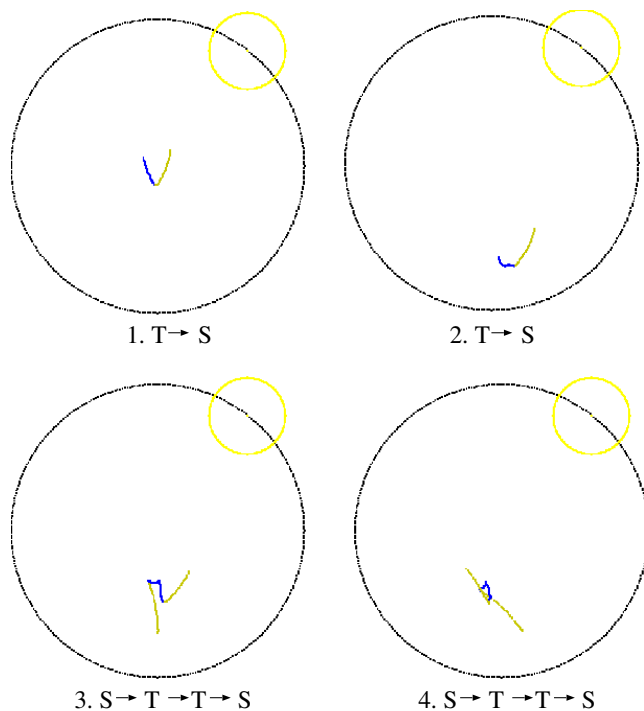


Fig. 5. Different types of trajectories resulting from the effects of noise

From the figure, it can be seen that the trajectories in red and green appeared when the robot was approaching toward the light source.

For comparison, we investigated navigation without sensory feedback. That is, the change over time of the sensory value is always zero, and the robot chose to either swim or tumble with constant probability ( $\frac{1}{2}$ ). This action selection should have let the robot do a random walk. The resulting trajectories are shown in Fig. 7. By comparing those trajectories, it can be seen that the robot changed its motion constantly for the random walk, while the robot sometimes made a long, consecutive swimming motion toward the light source under the proposed method.

In order to verify the phototaxis, we divided the circular field into two parts (area A-near half, and area B-far half in Fig. 6). The proportion of time spent in each area for each trial was calculated. The distribution of the proportion with average and standard deviation in ten trials for the proposed method and random walk is shown in Fig. 9. It can be clearly seen that the proportion of time spent in area A was higher than that in area B under the proposed method, while the distribution for the random walk does not show such a bias. By t-test, it was shown that the distribution under the proposed method is biased at a statistically significant level of 1%.

Additionally, we divided the circular field every 5[cm] into seven areas depending on the distance from the light source as shown in Fig. 9 in order to investigate the phototaxis in detail. The proportion of time spent in each was calculated for every trial. The distribution of the proportion was normalized with regard to the size of each area. This calculation

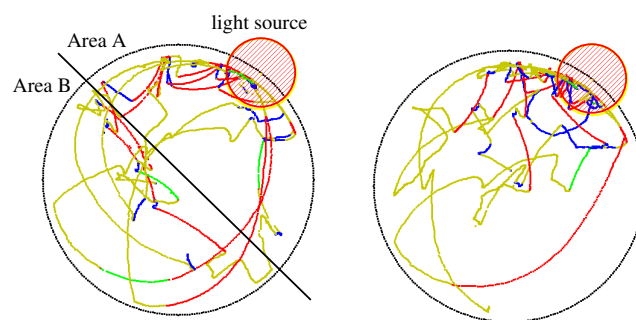


Fig. 6. Trajectories of robot under proposed method with phototaxis

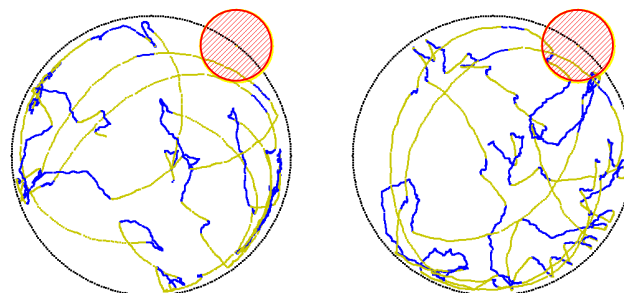


Fig. 7. Trajectories of robot in random walk

was performed in order to eliminate the effect of the size of each area, and the unit of the resulting distribution becomes  $[s/cm^2]$ . The average and standard deviation of the proportion in ten trials for the proposed method and random walk are shown in Fig. 9. It can be clearly seen that the proportion of time spent in areas near the light were higher than that in farther areas for the proposed method, while the distribution for the random walk does not show such a bias. The reason for having a large standard deviation in area 1 and 7 in both graphs in Fig. 9 is that their sizes are relatively small compared with other areas. The reason for having a higher possibility of being in area 1 in random walk in Fig. 9 the length of the wall of the tank is longer relative to the size of the area, which prevents the robot from moving farther away from the light.

4) *Comparison with Bacterial Motion:* The developed swimming robot exhibited phototaxis. However, actual bacteria show stronger phototaxis in the real world. The difference between the robot and a bacterium lies mainly in the scale of the world. The size of bacteria is usually 1-10[ $\mu m$ ], and the size of the developed swimming robot is 5[cm], which means there is a huge scale difference of  $10^4$ . At the bacterial scale, the noise in the environment such as the Brownian motion of surrounding water molecules is considerably large; thus the collision of water molecules with unbundled flagella enables a bacterium to frequently tumble.

Another difference is the Reynolds number of the fluid. The Reynolds number of the water flow past a bacterium is approximately  $10^{-5}$ , and that past the body of the robot we developed is approximately  $10^3$ . This indicates that viscosity is highly dominant over inertia in the bacterial world. That

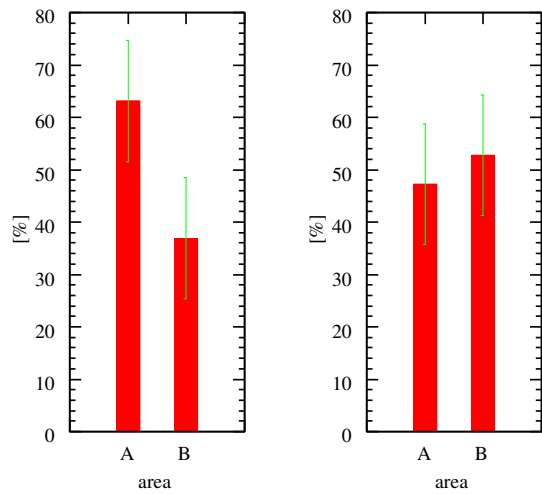


Fig. 8. Ratio of robot's presence in Area A and B for phototaxis and for random walk

is, bacteria can start moving and stop instantly, while the developed robot requires some time to start moving after the propeller screw begins rotating. This difference becomes significant especially when the robot is stuck in a narrow space such as a corner.

Since both the amplitude and the frequency of the environmental noise are relatively small, the degree of phototaxis for the developed robot is significantly low. However, the robot can intentionally generate a disturbed flow by taking advantage of large Reynolds number. It is impossible for a robot with only a 1-DOF motor to change its direction to explore in 2D space without the effect of such a noise. Therefore the robot can be regarded as making use of the noise to enhance its motility.

5) *Mathematical Explanation:* We also developed a simulation for the proposed method to explain the proposed method mathematically. In order to simplify the explanation, we consider a one dimensional case ( $1 \leq x \leq 500$ ) as shown in Fig. 10. The vertical axis indicates the orientation of the robot, which is either positive toward the signal source or negative. In the simulation, the source of the signal is assumed to exist at  $x = \infty$ , and the gradient of the signal is constant. Two parameters  $p$  and  $q$  are needed to explain the proposed method;  $p$  is the probability to switch direction and move forward one step when the robot is facing in the correct (positive) direction toward the signal source, and  $q$  is the probability to switch direction and move forward one step when the robot is facing in the wrong (negative) direction away from the signal source. Let  $\mathbf{p}_t$  denote the spatial probability distribution of the robot at each position and orientation at time  $t$  as follows:

$$\mathbf{p}_t = \begin{pmatrix} p_{1+} \\ p_{1-} \\ p_{2+} \\ p_{2-} \\ \vdots \\ p_{n-} \end{pmatrix},$$

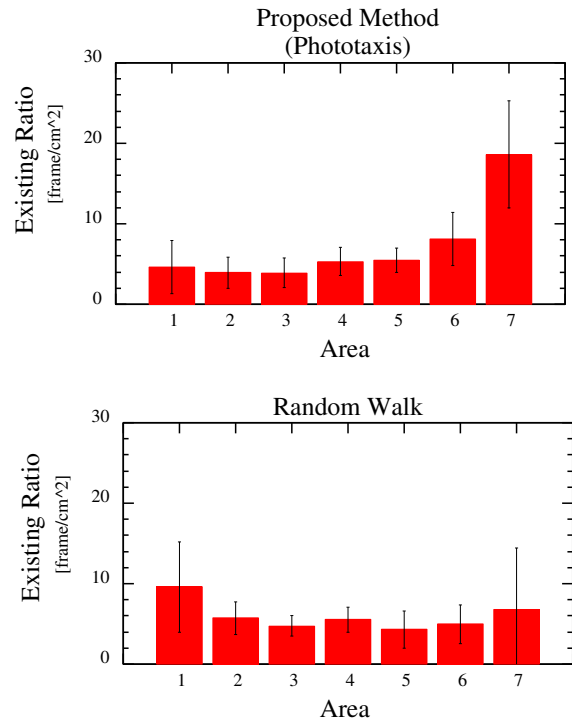
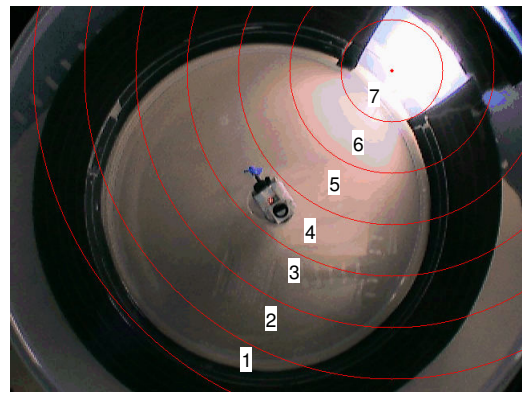


Fig. 9. Area division of experimental field for detailed evaluation, and resulting distribution of existing ratio of robot with phototaxis (top) and for random walk (bottom) in each area

then the temporal transition of the probability distribution can be expressed using the transition matrix  $\mathbf{T}$  as follows:

$$\mathbf{p}_{t+1} = \mathbf{T} \cdot \mathbf{p}_t$$

$$\mathbf{T} = \begin{pmatrix} p & 0 & 0 & 0 & \dots & 0 & 0 \\ 0 & 1-q & p & 1-q & \dots & 0 & 0 \\ 1-p & q & 0 & 0 & \dots & 0 & 0 \\ 0 & 0 & 0 & 0 & \dots & 0 & 0 \\ 0 & 0 & 1-p & q & \dots & 0 & 0 \\ \vdots & \vdots & \vdots & \vdots & \ddots & \vdots & \vdots \\ 0 & 0 & 0 & 0 & \dots & p & 1-p \\ 0 & 0 & 0 & 0 & \dots & 1-p & 0 \\ 0 & 0 & 0 & 0 & \dots & 0 & q \end{pmatrix}$$

We simulated the movement of the robot for 300 steps using  $p = 0.3$  and  $q = 0.8$ . For the initial condition, ten

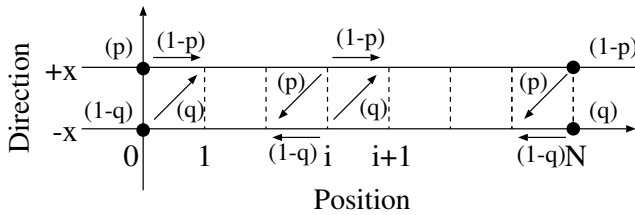


Fig. 10. State space for one-dimensional simulation

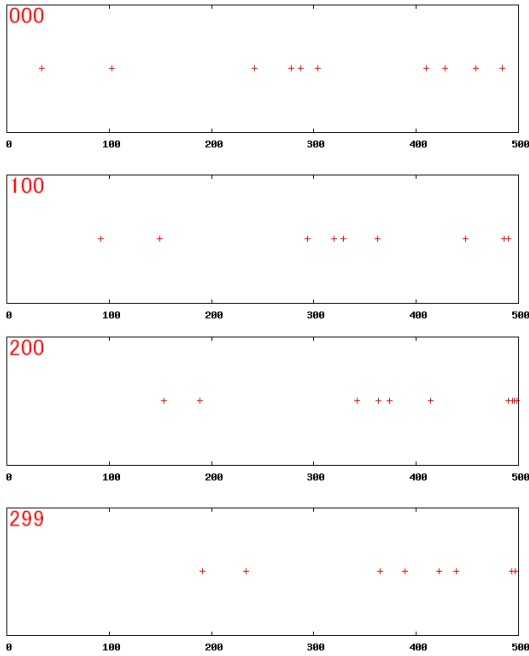


Fig. 11. Ten robots moving for 300 steps

robots were placed randomly facing random directions. The result of the simulation is shown in Fig. 11, where each point indicates the position of each robot and the number at the top left indicates the number of frames. From this figure, it can be seen that starting from random positions, all robots gradually converge toward the signal source.

The stationary probability distribution can be obtained by calculating the eigenvector associated with the maximum eigen value of the transition matrix  $T$ . By changing both the spacial resolution ( $n = 7$ ) and transition parameters ( $p = 0.3, q = 0.5$ ), the stationary probability distribution shown in Fig. 12 is obtained, which is similar to the experimental result shown in Fig. 9. This result implies that the strength of the phototaxis achieved by the developed robot can be expressed and evaluated by the parameters  $p, q$  in the transition matrix.

#### IV. CONCLUSION

In this paper, we described a small and simple, 1-DOF robot inspired by the mechanism for bacterial motion. The robot only has a single motor and a single sensor. The control strategy is to change the orientation due to various noises which exist in the environment, and also to change the frequency of turning in order to approach the goal. Experimental results indicated that the robot could statistically

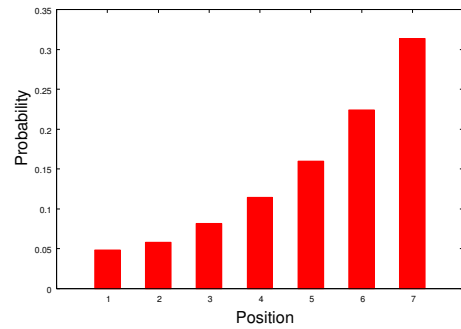


Fig. 12. Stationary probability distribution

approach the goal (light source) in two dimensional space with the 1-DOF actuator, which would be impossible for the robot to achieve without the utilization of noise. This mechanism should be able to be applied to realize robust robotic systems which can survive in severe environment.

Our future work includes further investigation of the relationship between the properties of the noise and the degree of taxis. The performance in complex environments should also be analyzed. We also aim to mathematically model the mechanism of taxis in 3D in order to clearly explain its properties, as well as to make use of it from the engineering point of view.

#### ACKNOWLEDGMENT

This research was supported by “Special Coordination Funds for Promoting Science and Technology: Yuragi Project” of the Ministry of Education, Culture, Sports, Science and Technology, Japan.

#### REFERENCES

- [1] M. Franz and H. Mallot, “Biomimetic Robot Navigation,” *Robotics and Autonomous System*, vol. 30, no. 1, pp. 133–153, 2000.
- [2] R. Moller, D. Lambrinos, R. Pfeifer, and R. Wehner, “Insect strategies of visual homing in mobile robots,” *Proc. Computer Vision and Mobile Robotics Workshop*, p. 141, 1998.
- [3] G. Bianco, R. Cassinis, A. Rizzi, N. Adami, and P. Mosna, “A bee-inspired robot visual homing method,” *eurobot*, p. 141, 1997.
- [4] R. Macnab, “Escherichia coli and salmonella: Cellular and molecular biology,” *American Society for Microbiology, Washington, D. C.*, vol. 2nd Ed. (Neidhardt, F. C. (editor-in-chief)), pp. 123–145, 1996.
- [5] S. H. Larsen, R. W. Reader, E. N. Kort, W. W. Tso, and J. Adler, “Change in direction of flagellar rotation is the basis of the chemotactic response in escherichia coli,” *Nature*, vol. 249, pp. 74–77, 1974.
- [6] Yukio Magariyama, “Difference between forward and backward swimming speeds of single polar-flagellated bacterium, *Vibrio alginolyticus*,” *EMS Microbiology Letters*, vol. 5, no. 205, pp. 343–347, 2001.
- [7] H. C. Berg and D. A. Brown, “Chemotaxis in escherichia coli analysed by three-dimensional tracking,” *Nature*, vol. 239, pp. 500–504, 1972.
- [8] R. M. Macnab, “The Gradient-Sensing Mechanism in Bacterial Chemotaxis,” *Proc. Nat. Acad. Sci. USA*, vol. 69, no. 9, pp. 2509–2512, 1972.
- [9] H. Ohtake, T. Yako, T. Tsuji, J. Kato, A. Kuroda, and M. Kaneko, “An approach to molecular artificial life: Bacterial intelligent behavior and its computer model,” *Workshop on Artificial Life V*, no. 673, pp. 362–368, 1996.
- [10] T. Tsuhi, A. Sakane, O. Fukuda, M. Kaneko, and H. Ohtake, “Biomimetic control of mobile robots based on a model of bacterial chemotaxis (in Japanese),” *Transactions of the Japan Society of Mechanical Engineers*, vol. 68-c, no. 673, pp. 2687–2694, 2002.